Neuronal Cell Death and Synaptic Pruning Driven by Spike-Timing Dependent Plasticity

Javier Iglesias[1,2,3] and Alessandro E.P. Villa[1,2,3]

[1] Information Systems Department, University of Lausanne, Switzerland
Javier.Iglesias@unil.ch
http://inforge.unil.ch/
[2] Laboratory of Neuroheuristics, University of Lausanne, Switzerland
http://www.nhrg.org/
[3] Inserm U318, Laboratory of Neurobiophysics, University Joseph Fourier,
Grenoble, France
Alessandro.Villa@ujf-grenoble.fr

Abstract. The embryonic nervous system is refined over the course of development as a result of two main processes: apoptosis (programmed cell death) and selective axon pruning. We simulated a large scale spiking neural network characterized by an initial apoptotic phase, driven by an excessive firing rate, followed by the onset of spike-timing-dependent plastiticity (STDP), driven by spatiotemporal patterns of stimulation. In the apoptotic phase the cell death affected the inhibitory more than the excitatory units. The network activity stabilized such that recurrent preferred firing sequences appeared along the STDP phase, thus suggesting the emergence of cell assemblies from large randomly connected networks.

1 Introduction

Genetic programs are assumed to drive the primordial pattern of neuronal connectivity through the actions of a limited set of trophic factors and guidance cues, initially forming excessive branches and synapses, distributed somewhat diffusely [9]. Then, refinement processes act to correct initial inaccuracies by pruning inappropriate connections while preserving appropriate ones. The embryonic nervous system is refined over the course of development as a result of the twin processes of cell death and selective axon pruning. Apoptosis – genetically programmed cell death – and necrosis – pathologic or accidental cell death due to irreversible damage – are two rough mechanisms for refining embryonic connections. However, the creation of complex connectivity patterns often requires the pruning of only a selected subset of the connections initially established by a neuron. Massive synaptic pruning following over-growth is a general feature of mammalian brain maturation [13]. Pruning starts near time of birth and is completed by time of sexual maturation. Quantitative analyses of synaptogenesis in the rat [1], the Rhesus monkey [3], and human [6] cortex have suggested a transient phase of high density of synapses during infancy.

Trigger signals able to induce synaptic pruning could be related to dynamic functions that depend on the timing of action potentials. Spike-timing-dependent synaptic plasticity (STDP) is a change in the synaptic strength based on the ordering of pre- and post-synaptic spikes. This mechanism has been proposed to explain the origin of long-term potentiation (LTP), i.e. a mechanism for reinforcement of synapses repeatedly activated shortly before the occurrence of a post-synaptic spike [2]. STDP has also been proposed to explain long-term depression (LTD), which corresponds to the weakening of synapses strength whenever the pre-synaptic cell is repeatedly activated shortly after the occurrence of a post-synaptic spike [11]. The relation between synaptic efficacy and synaptic pruning [4] suggests that the weak synapses may be modified and removed through competitive "learning" rules. Competitive synaptic modification rules maintain the average neuronal input to a post-synaptic neuron, but provoke selective synaptic pruning in the sense that converging synapses are competing for control of the timing of post-synaptic action potentials [14].

In this study the synaptic modification rule was applied to the excitatory-excitatory *(exc, exc)* and excitatory-inhibitory *(exc, inh)* connections. This plasticity rule might produce the strengthening of the connections among neurons that belong to cell assemblies characterized by recurrent patterns of firing. Conversely, those connections that are not recurrently activated might decrease in efficiency and eventually be eliminated. The main goal of our study is to determine whether or not, and under which conditions, such cell assemblies may emerge from a large neural network receiving background noise and content-related input organized in both temporal and spatial dimensions.

2   Model

The originality of our study stands on the application of an original bio-inspired STDP modification rule compatible with hardware implementation [5]. The complete neural network model is described in details elsewhere [7]. A sketch description of the model with specific model parameters related to the current study follows below.

10,000 integrate-and-fire units (80% excitatory and 20% inhibitory) were laid down on a 100×100 2D lattice according to a space-filling quasi-random Sobol distribution. Sparse connections between the two populations of units were randomly generated according to a two-dimensional Gaussian density function such that excitatory projections were dense in a local neighborhood, but probability long-range excitatory projections were allowed. Edge effects induced by the borders were limited by folding the network as a torus.

The state of the unit (spiking/not spiking) was a function of the membrane potential and a threshold. The states of all units were updated synchronously and the simulation was performed at discrete time steps corresponding to 1 ms. After spiking, the membrane potential was reset, and the unit entered an absolute refractory period lasting 3 and 2 time steps for excitatory and inhibitory units, respectively. For the simulation runs presented here each unit received a

background activity following an independent Poisson process and the "spontaneous" mean firing rate of the units was 5 spikes/s.

It is assumed *a priori* that modifiable synapses are characterized by discrete activation levels that could be interpreted as a combination of two factors: the number of synaptic *boutons* between the pre- and post-synaptic units and the changes in synaptic conductance. In the current study we attributed a fixed activation level (meaning no synaptic modification) $A_{ji}(t) = 1$, to *(inh, exc)* and *(inh, inh)* synapses while activation levels were allowed to take one of $A_{ji}(t) = \{0, 1, 2, 4\}$ for *(exc, exc)* and *(exc, inh)*, $A_{ji}(t) = 0$ meaning that the projection was permanently pruned out. For $A_{ji}(t) = 1$, the post-synaptic potentials were 0.84 mV and -0.8 mV for excitatory and inhibitory units, respectively.

The death of units by means of apoptosis is introduced in here, which is a major difference with preivous models [7]. A dead unit is characterized by the absence of any spiking activity. We define two mechanisms inducing cell death: the first is provoked by an excessive firing rate (apoptosis) and the second by the loss of excitatory inputs. For each unit at each time step, the mean firing rate computed over a window of 50 ms preceding the evaluation was compared to a threshold value of 245 and 250 spikes/s for excitatory and inhibitory units, respectively. If the rate exceeded the threshold, then the unit had a probability of entering apoptosis determined by the function

$$P_{\text{apoptosis}}(t) = \frac{0.5 \cdot t^2 - 4.5 \cdot 10^{-6} \cdot t^3}{44 \cdot (2.5 \cdot 10^6 + 6 \cdot 10^{-3} \cdot t^2)}. \tag{1}$$

with $P_{apoptosis}(t = 100) = 4.5 \cdot 10^{-5}$, $P_{apoptosis}(t = 700) = 2.2 \cdot 10^{-3}$, and $P_{apoptosis}(t = 800) = 2.9 \cdot 10^{-3}$. The apoptosis could be induced according to this mechanism during an initial phase lasting 700 or 800 simulation time steps. After this intial phase, the timing of the pre- and post-synaptic activity started driving the synaptic plasticity through the STDP rule. Due to this plasticity, the projections from and to "dead" units underwent a slow activation level decay finally leading to their pruning when $A_{ji}(t) = 0$. "Dead" projections were thus pruned along with others by the action of STDP and some units were found without any excitatory input left. The loss of excitatory inputs provoked the cell death and these units stopped firing (even in presence of background activity) immediately after the pruning of the last excitatory input synapse.

3   Simulations

Each simulation run lasted 10^5 discrete time steps (1 ms per time step), corresponding to a duration of about 2 minutes. After a stabilization period of 1000 ms without any external input, a 100 ms long stimulus was presented every 2000 ms. Overall this corresponds to 50 presentations of the stimulus along one simulation run. Before the simulation started, two sets of 400 excitatory units were randomly selected from the 8,000 excitatory units of the network, labeled sets A and B. Each set was divided into 10 groups of 40 units, $A = \{A_1, A_2, \ldots, A_{10}\}$ and $B = \{B_1, B_2, \ldots, B_{10}\}$. At each time step during a stimulus presentation,
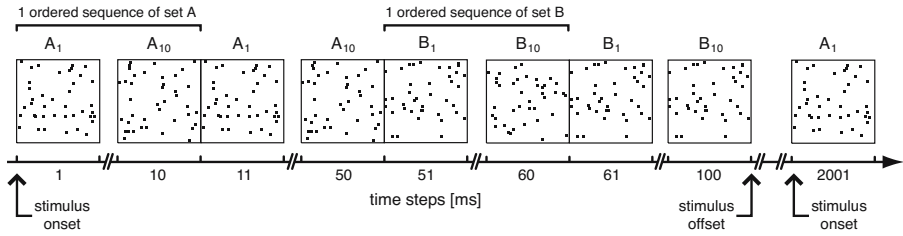
**Fig. 1.** Example of one AB stimulus presentation

the 40 units of one group received a large excitatory input on their membrane, leading to their synchronous firing. The 10 groups of a set were stimulated following an ordered sequence, thus defining a reproducible spatiotemporal stimulus composed by the repetition of sequences lasting 10 ms each (see Fig. 1). A random, equiprobable mix of the two stimuli composed by either $5\times$ sequence A followed by $5\times$ sequence B (AB) or $5\times$ sequence B followed by $5\times$ sequence A (BA) was presented.

At time t=100 s, the units, characterized by more than four active excitatory input projections that did not belong to the sets of stimulated units A or B, were selected. For each of these selected units, the spikes produced by the independent Poisson background process were discarded from their spike trains to extract the so-called "effective spike trains". Thus, the effective spike trains correspond to the true network activity. The first 1000 ms of activity were discarded because this interval corresponds to the apoptosis phase. These effective spike trains were searched for the occurrence of spatiotemporal firing patterns [16], as described in the following section.

3.1   Time Series Analysis

Spatio-temporal firing patterns (often referred to as "preferred firing sequences") are defined as sequences of intervals with high temporal precision (of the order of few ms) between at least 3 spikes (of the same or different units) that recur at levels above those expected by chance [17]. The pattern detection algorithm begins with finding all single or multineuron sequences of intervals that repeat two or more times within a record. Secondly, the algorithm computes how many of such sequences of intervals can be expected by chance and provides confidence limits for this estimation. The "pattern grouping algorithm"[1] [16] performs clusterization into one group of sequences of intervals with slight difference in spike timing. Figure 2 illustrates the outline of this method. For the present study, the pattern grouping algorithm was used to find patterns of at least three spikes (triplets), with a minimal significance level of 10%, repeating at least 7 times in the interval [1-100] s, provided the entire pattern lasted not more than 800 ms and was repeated with an accuracy of less than ± 5 ms.

---

[1] http://OpenAdap.net/
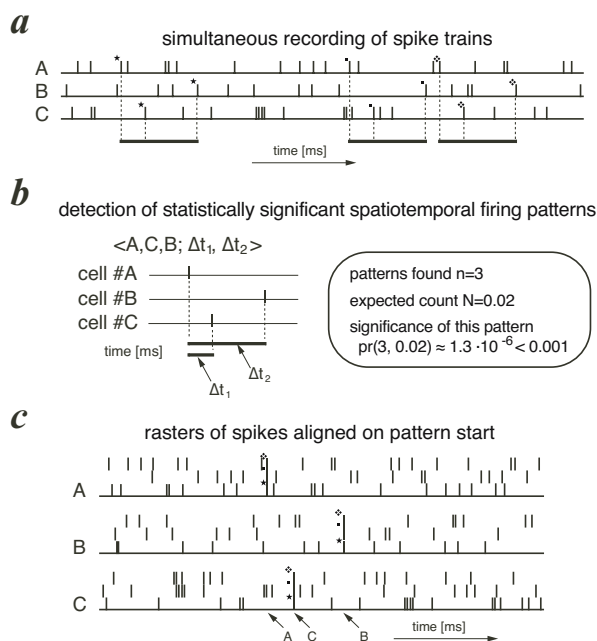
Fig. 2. Outline of the general procedure followed by pattern detection algorithms. **(a)**: Analysis of a set of simultaneously recorded spike trains. Three cells, labeled A, B, and C, participate to a patterned activity. Three occurrences of a precise pattern are detected. Each occurrence of the pattern has been labeled by a specific marker in order to help the reader to identify the corresponding spikes. **(b)**: Estimation of the statistical significance of the detected pattern. **(c)**: Display of pattern occurrences as a raster plot aligned on the pattern start.

4   Results

4.1   Firing Rate-Induced Apoptosis

Figure 3 shows the evolution of the number of excitatory and inhibitory units during the first simulated second. For the first 800 time steps, units with mean firing rates exceeding the threshold entered apoptosis with the probability expressed by $P_{\mathrm{apoptosis}}(t)$. It is possible to linearly fit the cell death dynamics with the probability function suggesting that the inhibitory units enter the apoptosis process about 70 ms before the excitatory units. After the end of this initial phase, STDP-driven synaptic pruning could modify the synaptic weights, thus inducing cell death due to the loss of excitatory inputs at a longer time-scale that is not depicted in Figure 3.

The initial apoptosis phase prevented the network from entering overactivity due to saturation by inducing the death of those units that tended to have an exceeding activity since the early steps of the simulation. These units are known to destabilize the network and ignite the saturation. The addition of this feature
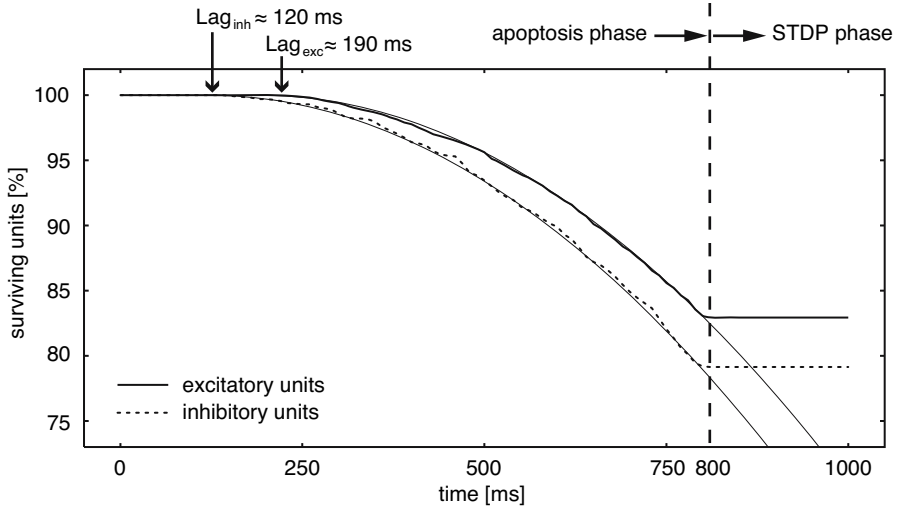
Fig. 3. Ratio of surviving units as a function of time with respect to initial conditions: 8000 excitatory units (plain line) and 2000 inhibitory units (dotted line). In this simulation, firing rate-induced apoptosis was stopped after 800 time steps. Thin lines correspond to the probability function $P_{\mathrm{apoptosis}}(t)$ with lags.

to the model greatly improved the stability of the network while maintaning its ability to produce spatiotemporal firing patterns.

4.2   Spatiotemporal Firing Patterns

In two different simulations, firing rate-induced apoptosis was stopped after 700 or 800 time steps. The first condition lead to a larger number of surviving units at t=100 s with lower mean firing rates than in the second condition. Spatiotemporal firing patterns were searched for in both conditions. Two patterns involving a single excitatory unit are described in more details in Figure 4 and Figure 5.

The pattern <79,79,79; 453±3.5, 542±2.5> was composed by spikes produced by a single unit labeled here #79 (Fig. 4a). This notation means that the pattern starts with a spike of unit #79, followed 453±3.5 ms by a second spike of the same unit, and followed by a third spike 542±2.5 ms after the first. Between t=1 and t=100 seconds, 51 repetitions of the pattern were observed. The statistical significance of this pattern was $7.5 \cdot 10^{-4}$. No correlation could be found between the timing of the spatiotemporal pattern and the stimulation onset (Fig. 4b). Figure 4c shows that the occurrences of the pattern onset along the simulation. The pattern occurred 23 times between $1 < t < 25$ seconds, 13 times between $25 < t < 50$ seconds, and 15 times between $50 < t < 100$ seconds. This might suggest that the network dynamics giving rise to the pattern was slowly disrupted by the continuous STDP-driven pruning.

The pattern <13,13,13; 234±3.5, 466±4.5> was composed by spikes produced by a single unit labeled here #13 (Fig. 5a). This notation means that the pattern
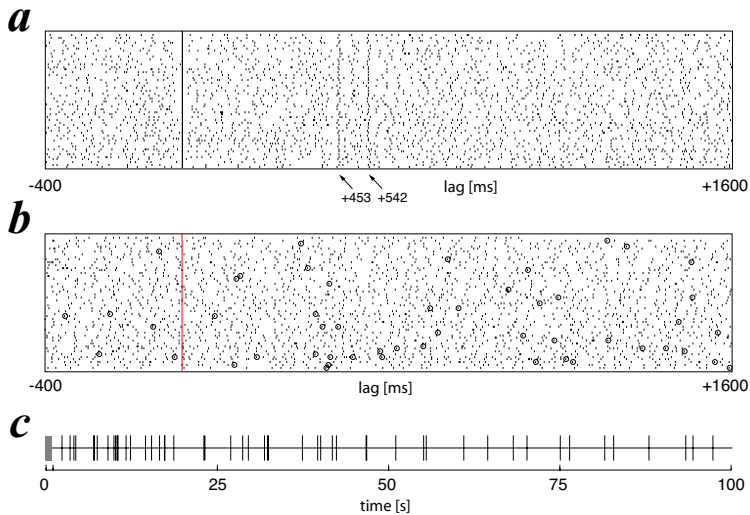
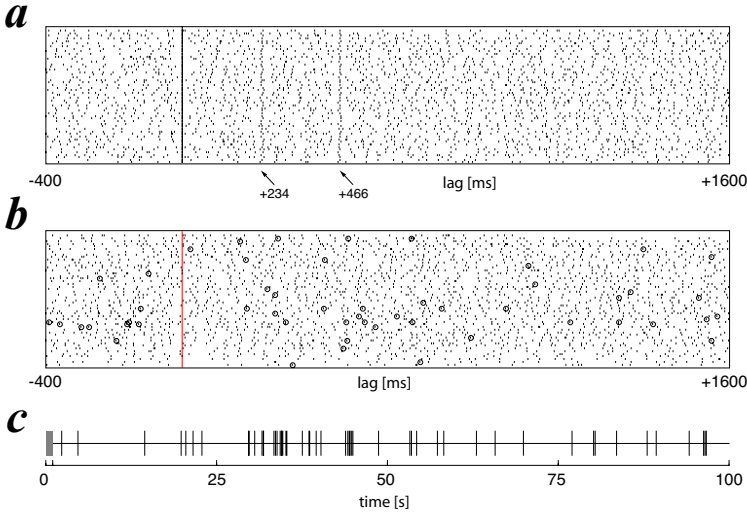**Fig. 4.** Spatiotemporal pattern <79,79,79; 453±3.5, 542±2.5>. **(a)**: Raster plot showing the 51 repetitions of the pattern aligned on the pattern start; **(b)**: Raster plot showing the activity of unit #79 aligned on the stimulus onset: each start event of a pattern occurrence is marked by a circle; **(c)**: Pattern occurrence timing plot: each vertical tick represents the start event of a pattern occurrence.

starts with a spike of unit #13, followed 234±3.5 ms by a second spike of the same unit, and followed by a third spike 466±4.5 ms after the first. Between t=1 and t=100 seconds, 52 repetitions of the pattern were observed. The statistical significance of this pattern was $3.4 \cdot 10^{-3}$. No correlation could be found between the timing of the spatiotemporal pattern and the stimulation onset (Fig. 5b). Figure 5c shows that the pattern occurred 7 times between $1 < t < 25$ seconds, 27 times between $25 < t < 50$ seconds, 8 times between $50 < t < 75$ seconds, and 10 times between $75 < t < 100$ seconds. This might suggest that the changes in the network dynamics induced by the continuous STDP-driven pruning lead to a transient state between $25 < t < 50$ seconds when the appearance of this pattern is favored.

5   Discussion

We simulated a large scale spiking neural network, with the time resolution of 1 ms, characterized by a brief initial apoptotic phase that extended our previous model [7]. During this phase the units that exceeded a certain threshold of firing had an increasing probability to die with the passing of time until 700 (or 800, depending on the simulation runs) time units. The inhibitory units entered the apoptosis process about 70 ms before the excitatory units. The death dynamics of both populations followed the probabilty function to die with only minor deviations. After the stop of the apoptosis, spike-timing-dependent plasticity

Fig. 5. Spatiotemporal pattern <13,13,13; 234±3.5, 466±4.5>. **(a)**: Raster plot showing the 52 repetitions of the pattern aligned on the pattern start; **(b)**: Raster plot showing the activity of unit #13 aligned on the stimulus onset: each start event of a pattern occurrence is marked by a circle; **(c)**: Pattern occurrence timing plot: each vertical tick represents the start event of a pattern occurrence.

(STDP) and synaptic pruning were made active. Selected sets of units were activated by regular repetitions of a spatiotemporal pattern of stimulation. During the STDP phase, the cell death could occur only if a unit became deafferented, i.e. it looses all its excitatory afferences because of synaptic pruning.

We recorded the spike trains of all excitatory units that were not directly stimulated and that were surviving at the arbitrary end of the simulation set at $t = 100$ seconds. In these spike trains we searched for preferred firing sequences that occurred beyond random expectation [16] and we found evidence of their appearance. We suggest that the detection of such preferred firing sequences might be associated with the emergence of cell assemblies from the initially locally connected random network [8]. The addition of cell death to the model improved the stability of the network over our previous studies while maintaining its ability to let emerge cell assemblies associated to preferred firing sequences. The self-organization of spiking neurons into cell assemblies was recently reported in other studies of large simulated networks connected by STDP-driven projections [10]. These authors emphasized the emergence of spontaneously self-organized neuronal groups, even in absence of correlated input, associated with the spatiotemporal structure of firing patterns, if axonal conduction delays and STDP were incorporated in the model.

Our simulation results offer also the ground of testing several hypothesis with respect to neuroanatomical experimental results. Indeed, there is an increasing interest in investigating the cortical circuits and their synaptic connectivity with

a statistical approach related to the graph theory. Results obtained from layer 5 neurons in the visual cortex of developping rats [15] indicate that many aspects of the connectivity patterns differ from random networks. In particular, the distribution of synaptic connection strength in those cortical circuits show an overrepresentation of strong synaptic connections correlated with the overrepresentation of some connectivity patterns. The authors [15] suggest that the local cortical network structure could be viewed as a skeleton of stronger connections in a sea of weaker ones.

The spike-timing-dependent plasticity rule implemented in our simulation has already been successfully implemented and tested in the POEtic tissue [5]. This electronic circuit is a flexible hardware substrate showing the basic features that permit living beings to show evolutionary, developmental or learning capabilities [12]. In future work, we intend to use the POEtic tissue in the investigation of the role of apoptosis and synaptic pruning in the unsupervised shaping of large simulated neural networks. The genomic features of the POEtic tissue offer the possibility to implement the programmed cell death in simulations of large spiking neural networks. It is expected that the computational power of the dedicated plateform will ease the simulation of larger networks to explore the impact of their size on the dynamics.

References

1. Aghajanian, G. K. and Bloom, F. E.: The formation of synaptic junctions in developing rat brain: A quantitative electron microscopic study. Brain Research **6**:4 (1967) 716–27

2. Bi, G. Q. and Poo, M. M.: Synaptic modifications in cultured hippocampal neurons: dependence on spike timing, synaptic strength, and postsynaptic cell type. J Neurosci. **18** (1998) 10464-72

3. Bourgeois, J. and Rakic, P.: Changes of synaptic density in the primary visual cortex of the macaque monkey from fetal to adult stage. Journal of Neuroscience **13** (1993) 2801–20

4. Chechik, G., Meilijson, I. and Ruppin, E.: Neuronal Regulation: A Mechanism for Synaptic Pruning During Brain Maturation. Neural Computation **11** (1999) 2061–80

5. Eriksson, J., Torres, O., Mitchell, A., Tucker, G., Lindsay, K., Rosenberg, J., Moreno, J.-M. and Villa, A.E.P.: Spiking Neural Networks for Reconfigurable POEtic Tissue. Lecture Notes in Computer Science **2606** (2003) 165–74

6. Huttenlocher, P.R.: Synaptic density in human frontal cortex – Developmental changes and effects of aging. Brain Research **163**:2 (1979) 195–205

7. Iglesias, J., Eriksson, J., Grize, F., T., Marco and Villa, A.E.P.: Dynamics of Pruning in Simulated Large-Scale Spiking Neural Networks. Biosystems **79** (2005) 11–20

8. Iglesias, J., Eriksson, J., Pardo, B., Tomassini, M. and Villa, A.E.P.: Stimulus-Driven Unsupervised Pruning in Large Neural Networks. Lecture Notes in Computer Science **3704** (2005) 59–68
9. Innocenti, G. M.: Exuberant development of connections, and its possible permissive role in cortical evolution. Trends in Neurosciences **18**:9 (1995) 397–402
10. Izhikevich, E. M., Gally, J. A. and Edelman, G. M.: Spike-timing Dynamics of Neuronal Groups. Cerebral Cortex **14** (2004) 933–44
11. Karmarkar, U. R. and Buonomano, D. V.: A model of spike-timing dependent plasticity: one or two coincidence detectors? J Neurophysiol. **88** (2002) 507–13
12. Moreno, J. M., Eriksson, J. L., Iglesias, J. and Villa A. E. P.: Implementation of Biologically Plausible Spiking Neural Networks Models on the POEtic Tissue. Lecture Notes in Computer Science **3637** (2005) 188–97
13. Rakic, P., Bourgeois, J. P., Eckenhoff, M. F., Zecevic, N. and Goldman-Rakic, P. S.: Concurrent overproduction of synapses in diverse regions of the primate cerebral cortex. Science **232** (1986) 232–5
14. Song, S. and Abbott, L.F.: Cortical Development and Remapping through Spike Timing-Dependent Plasticity. Neuron **32** (2001) 339–50
15. Song, S., Sjöström, P.J., Reigl, M., Nelson, S. and Chklovskii, D.B.: Highly Nonrandom Features of Synaptic Connectivity in Local Cortical Circuits. PLoS Biology **3**:3 (2005) 0507–19
16. Tetko, I. V. and Villa, A. E.: A pattern grouping algorithm for analysis of spatiotemporal patterns in neuronal spike trains. 1. Detection of repeated patterns. Journal of Neuroscience Methods **105** (2001) 1–14
17. Villa, A. E. P.: Empirical Evidence about Temporal Structure in Multi-unit Recordings. Time and the Brain, Chapter 1, Editor: R. Miller, Harwood Academic Publishers (2000) 1–51